Fish and Shellfish Immunology 89 (2019) 448–457

Contents lists available at ScienceDirect

Fish and Shellfish Immunology

journal homepage: www.elsevier.com/locate/fsi

Full length article

Characterization and functional analysis of a novel mannose-binding lectin from the swimming crab *Portunus trituberculatus*

Mengjie Zhang[a,c,d,1], Yuan Liu[a,b,c,1], Chengwen Song[a,b,c], Junhao Ning[a,c,d], Zhaoxia Cui[e,b,*]

[a] CAS Key Laboratory of Experimental Marine Biology, Institute of Oceanology, Chinese Academy of Sciences, Qingdao 266071, China
[b] Laboratory for Marine Biology and Biotechnology, Qingdao National Laboratory for Marine Science and Technology, Qingdao, 266071, China
[c] Center for Ocean Mega-Science, Chinese Academy of Sciences, Qingdao, 266071, China
[d] University of Chinese Academy of Sciences, Beijing, 100049, China
[e] School of Marine Science, Ningbo University, Zhejiang, Ningbo, 315211, China

ARTICLE INFO

Keywords:
Portunus trituberculatus
Mannose-binding lectin
Pattern recognition receptor
Antimicrobial activities

ABSTRACT

Mannose-binding lectin (MBL) is a pattern recognition receptor (PRR) that plays an important role in the innate immune response. In this study, a novel mannose-binding lectin was cloned from the swimmimg crab *Portunus trituberculatus* (designated as PtMBL). The complete cDNA of PtMBL gene was 1208 bp in length with an open reading frame (ORF) of 732 bp that encoded 244 amino acid proteins. PtMBL shared lower amino acid similarity with other MBLs, yet it contained the conserved carbohydrate-recognition domain (CRD) with QPD motif and was clearly member of the collectin family. PtMBL transcripts were mainly detected in eyestalk and gill with sexually dimorphic expression. The temporal expression of PtMBL in hemocytes showed different activation times after challenged with *Vibrio alginolyticus*, *Micrococcus luteus* and *Pichia pastoris*. The recombinant PtMBL protein revealed antimicrobial activity against the tested Gram-negative and Gram-positive bacteria. It could also bind and agglutinate (Ca^{2+}-dependent) both bacteria and yeast. Furthermore, the agglutinating activity could be inhibited by both D-galactose and D-mannose, suggesting the broader pathogen-associated molecular patterns (PAMPs) recognition spectrum of PtMBL. These results together indicate that PtMBL could serve as not only a PRR in immune recognition but also a potential antibacterial protein in the innate immune response of crab.

1. Introduction

As the invertebrates, crustaceans lack an acquired immune system and solely rely on innate immune system to defense against the invading pathogens [1]. Immune recognition is the primary and crucial step in discriminating self and non-self in innate immune response [2]. It is initiated by pattern recognition receptors (PRRs) to recognize pathogen-associated molecular patterns (PAMPs) on the surface of microbes [3]. Among the variety of PRRs, C-type lectins, a superfamily of Ca^{2+}-dependent carbohydrate-recognition protein containing at least one carbohydrate recognition domain (CRD), have been identified as potentially important effectors in crustacean immune defense [4,5].

Mannose-binding lectin (MBL), a member of C-type lectin, can recognize and bind to terminal mannose residues on the surface of pathogens and initiate the lectin complement pathway in vertebrates [6–10]. MBL belongs to the collectin family of proteins, and consists of a cysteine-rich N-terminal region, a collagen-like domain, a neck region and the C-terminal CRD [11,12]. The collagen-like domain is supposed to interact with MBL-associated serine proteases (MASPs) to form a complex in complement activation [13]. Based on an EPN (Glu-Pro-Asn) motif in the CRD region, the major ligands of vertebrate MBLs are D-mannose, L-fucose and *N*-acetyl-D-glucosamine (GlcNAc) [14,15]. However, the motif for ligand binding is of great diversity in invertebrates. For example, EPD (Glu-Pro-Asp), QPG (Gln-Pro-Gly), QPS (Gln-Pro-Ser), YPG (Tyr-Pro-Gly), and YPT (Tyr-Pro-Thr) were found in the corresponding sites of the specific motif [16].

Several MBLs have been identified in crustaceans, and most play a crucial role in innate immune defense against a wide range of microbes. For example, mannose receptor from crayfish *Procambarus clarkii* (PcMR) is involved in the innate immune response against bacterial pathogens [17]. Pl-MBL from crayfish Pacifastacus leniusculus may interfere with the LPS-induced activation of the proPO-system [18]. MrMBL-N20 and MrMBL-C16 peptides, deriving from MrMBL of prawn *Macrobrachium rosenbergii*, are important antimicrobial peptides for the

* Corresponding author. School of Marine Science, Ningbo University, Zhejiang, Ningbo, 315211, China.
E-mail address: cuizhaoxia@nbu.edu.cn (Z. Cui).
[1] These authors contributed equally to this work.

https://doi.org/10.1016/j.fsi.2019.04.007
Received 20 January 2019; Received in revised form 6 March 2019; Accepted 3 April 2019
Available online 08 April 2019
1050-4648/ © 2019 Published by Elsevier Ltd.

recognition and eradication of viral and bacterial pathogens [19]. Moreover, several C-type lectins containing EPN motif could display anti-WSSV and anti-bacteria activities, such as LvCTL from *Litopenaeus vannamei* [20], FcLec5 from *Fenneropenaeus chinensis* [21] and FmLec2 from *Fenneropenaeus merguiensis* [22]. However, the functions of MBLs in crab immunity remain unclear.

The swimming crab *Portunus trituberculatus* is important commercial crustacean, and support the large crab fishery and aquaculture in China with the total yield exceeding 120,000 tons in 2017 [23]. Crabs live in an aquatic environment full of bacteria, fungi and other potential pathogens. Improving knowledge of the innate immunity in crab will be useful in diseases control in crab aquaculture. In this study, the full-length cDNA of MBL from *P. trituberculatus* (designated as PtMBL) was cloned. The tissue distribution of PtMBL transcripts and their temporal response to microbes challenge were examined. In addition, the functions of the recombinant PtMBL protein were investigated by antimicrobial activity, binding activity and microbial agglutination assay.

2. Materials and methods

2.1. Crabs, immune challenge and samples collection

Healthy *P. trituberculatus* averaging (150 ± 10) g in weight were collected from Qingdao, China, and acclimated at 16 ± 1 °C for 1 week before processing. During the experiment, the crabs were fed with clam meat once daily at night. For pathogens challenge experiment, 84 crabs were employed, randomly divided into 4 groups (21 individuals each group) and kept in aerated tanks. Three groups of crabs were injected 100 μl live *Vibrio alginolyticus* (3×10^8 CFU mL^{-1}), *Micrococcus luteus* (1×10^8 CFU mL^{-1}) and *Pichia pastoris* (4×10^7 CFU mL^{-1}) suspended in 0.1 moL/L PBS (pH 7.0) at the arthrodial membrane of the last walking leg, respectively. The last group of crabs receiving an injection of 100 μl PBS was served as the control group. The remaining untreated crabs were used as blank. The injected crabs were returned to the water tanks, and three individuals were randomly sampled at the time point of 2, 4, 8, 12, 24, 48 and 72 h post-injection.

The haemolymph was harvested from the last walking leg using a syringe and quickly added to an equal volume of anticoagulant modified Alsever solution (27 mM sodium citrate, 336 mM NaCl, 115 mM glucose, 9 mM EDTA, pH 7.0) [24]. Samples were immediately centrifuged at 800 g, 4 °C for 5 min to collect the hemocytes. Hemocytes, gill, hepatopancreas, eyestalk, muscle, heart, intestine, stomach, thoracic ganglion, brain and ovary or testis from five untreated female and male crabs were collected to determine the tissue distribution of PtMBL transcripts.

2.2. RNA isolation, cDNA synthesis and cloning the full-length cDNA of PtMBL

The total RNA was extracted from the samples of *P. trituberculatus* using TRIzol reagent according to the manufacture's protocol (Invitrogen). The first-strand cDNA was synthesized for the quantitative real-time PCR (qRT-PCR) analysis using a PrimeScript™ first Strand cDNA Synthesis Kit (Takara, Dalian, China) with an oligo dT primer. To amplify the 3′ end of PtMBL cDNA sequence, the first-strand cDNA was synthesized using the Clonetech SMARTer™ RACE cDNA Amplification kit (Takara, Dalian, China) with 3′-CDS Primer (3′-RACE CDS Primer).

A gene specific forward primer PtMBL-3′F (Table 1) was designed based on the unigene sequence obtained from transcriptome data. 3′ fragment was amplified using PtMBL-3′F and 3′ RACE Outer Primer (3′ ROP). And then a pair of primers, PtMBL-F and PtMBL-R (Table 1) was designed to obtain the ORF fragment of the cDNA sequence. The polymerase chain reaction (PCR) was performed in a 25 μl reaction volume containing 17.3 μl sterile distilled H_2O, 2.5 μl of 10 × PCR buffer, 2.0 μl of dNTP (10 Mm), 1 μl of each primer (5 mM), 0.2 μl (1 U) of Taq polymerase (TaKaRa), and 1 μl of DNA template (approximately 30 ng). The PCR was conducted under the following parameters: 94 °C for 3 min, followed by 35 cycles of 94 °C for 30 s, 57 °C for 50 s, and 72 °C for 1 min, and finally 72 °C for 10 min. The amplifications were performed on TaKaRa PCR Thermal Cycler Dice Model TP600 (Takara Bio Inc.) The PCR products were gel-purified and cloned into pMD19-T simple vector (TaKaRa). After being transformed into the competent cells of *Escherichia coli* DH5α, the positive recombinants were identified through anti-Amp selection and PCR screening with M13-47 and RV-M primers (Table 1). Three of the positive clones were sequenced by a commercial company (Sangon, China). The complete PtMBL cDNA sequence was obtained by overlapping the two fragments.

2.3. Sequence analysis, tertiary structures prediction and phylogenetic analysis

Blast algorithm at National Center for Biotechnology Information (http://www.ncbi.nlm.gov/blast/) was used to search the homology of nucleotide and protein sequences. The deduced amino acid sequence was analyzed with the Expert Protein Analysis System (http://www.expasy.org/). SignalP 4.1 program was utilized to predict the presence and location of signal peptide, and the cleavage sites in amino acid sequences (http://www.cbs.dtu.dk/services/SignalP/). Scanprosite program was utilized to predict the potential disulfide bonds and their position (http://www.expasy.ch/tools/scanprosite/). The carbohydrate recognition domain (CRD) and glycosylation sites were predicted using ExPASy PROSITE (http://www.expasy. ch/prosite/). A homology model of PtMBL was constructed using SWISS-MODEL (http://swissmodel.expasy.org) and verified by Swiss-PdbViewer. The ClustalW Multiple Alignment program (http://www.ebi.ac. uk/clustalw/) was used to create the multiple sequence alignment. An unrooted phylogenetic tree was constructed based on the aligned amino acid sequences by the neighbour-joining (NJ) algorithm embedded in MEGA 7 program. The reliability of the branching was tested by 1000 bootstraps.

2.4. Quantitative analysis of PtMBL expression

The mRNA expression of PtMBL transcripts in various tissues, including hemocytes, gill, hepatopancreas, eyestalk, muscle, heart, intestine, stomach, thoracic ganglion, ovary, testis and brain of untreated crabs, and the temporal expression of PtMBL transcripts in hemocytes of crabs challenged with *V. alginolyticus, M. luteus and P. pastoris* were determined by quantitative real-time PCR. The cDNA was diluted 100 times by DEPC-treated water for the next step. The SYBR Green RT PCR assay was carried out in an ABI PRISM 7300 Sequence Detection System (Applied Biosystems).

A pair of gene-specific primers (MBL-RTF and MBL-RTR, see Table 1) was used to amplify a product of 165 bp PtMBL gene. The β-actin from *P. trituberculatus* [25], amplified with primers Actin-F and Actin-R (Table 1), was chosen as reference gene for internal standardization. DEPC-water for the replacement of cDNA template was used as negative control. Reactions were carried out on an ABI PRISM 7300 Sequence Detection System (Applied Biosystems) using SYBR green II as fluorescent dye. The PCR was carried out in a total volume of 10 μl, containing 3.33 μl of 2 × SYBR Premix Ex Taq (TaKaRa), 0.13 μl 50 × ROX Reference Dye, 4 μl of the diluted cDNA mix, 0.13 μl of each primer (10 mM) and 2.27 μl sterile distilled H_2O. The thermal profile for SYBR Green RT PCR was 95 °C for 30 s, followed by 40 cycles of 95 °C for 5 s and 60 °C for 35 s. After the PCR program, data were analyzed with ABI7300 SDS software (Applied Biosystems). Fold change for the gene expression relative to controls was determined by the $2^{-\Delta\Delta Ct}$ method [26]. All data were given in terms of relative mRNA expression as mean ± S.E. The results were subjected to one way analysis of variance (one way ANOVA) using SPSS 16.0, and the *P* values less than 0.05 and 0.01 were considered statistically significant.

Table 1
Primers used in this study.

Primers Name	Sequence (5′–3′)	PCR objective
PtMBL-F	TTCTCCTCCGCAAGATGAAGGTC	Gene cloning
PtMBL-R	GGACAGTCACTATCTCCGAACCTATT	Gene cloning
PtMBL-3′F	CTGGCAATGGCTGGATGGAAGTT	Gene cloning
3′ROP	GACTCGAGTCGATCGATTTTTTTTTTTTTTTTT	Gene cloning
PtMBL-RTF	CTGGAGTTGGTGTTGGGAATA	Real-time PCR
PtMBL-RTR	TTGTCTTCATCCCTACTTTCG	Real-time PCR
Actin-F	TCACACACTGTCCCCATCTACG	Real-time PCR
Actin-R	ACCACGCTCGGTCAGGATTTTC	Real-time PCR
PtMBL-REF	CGGGATCCTCCCGGCGTCCCTACCCGAG	Recombinant expression
PtMBL-RER	CCCTCGAGTTAACCATACTGGGGCACGG	Recombinant expression
M13–47	CGCCAGGGTTTTCCCAGTCACGAC	Sequencing
T7 promoter	TAATACGACTCACTATAGGG	Sequencing
T7 terminator	GCTAGTTATTGCTCAGCGGT	Sequencing

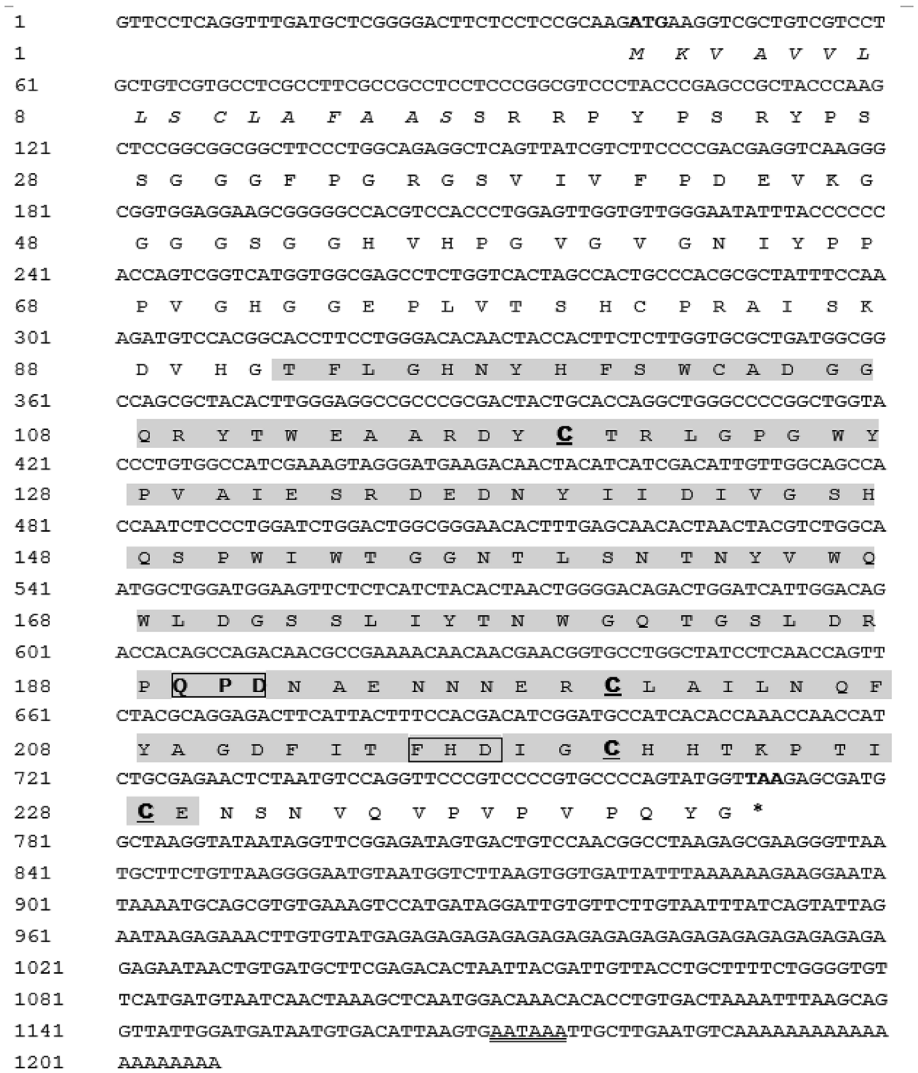

Fig. 1. Complete nucleotide and deduced amino acid sequence of PtMBL. The start codon (ATG) is represented as M, while the stop codon (TAA) is in bold and marked with asterisk. Putative signal peptide sequence is shown in italics. One CRD region is shown in the shadow (positions 92–229). The QPD motif that is important for the ligand-binding specificity is shown in bold letters and boxed. A FHD motif for Ca^{2+} binding site is boxed. Four cysteine residues that are involved in the formation of two disulfide bonds in CRD are shown in bold letters and underlined. A polyadenylation consensus signal (AATAAA) is shown in double-underlined.

2.5. The construction of recombinant plasmids

A pair of gene-specific primers, PtMBL-REF and PtMBL-RER, was designed to amplify the sequence encoding mature peptide of PtMBL (*Bam*H I and *Xho* I sites are underlined in Table 1). The purified PCR products were inserted into pMD19-T simple vector and then were sequenced to ensure the correct coding sequence. The recombinant plasmid pMD19-T-PtMBL digested completely by restriction enzymes *Bam*H I and *Xho* I (NEB), and then cloned into pET-32a (+) vector (Novagen). Afterward, the recombinant plasmid pET-32a-PtMBL was

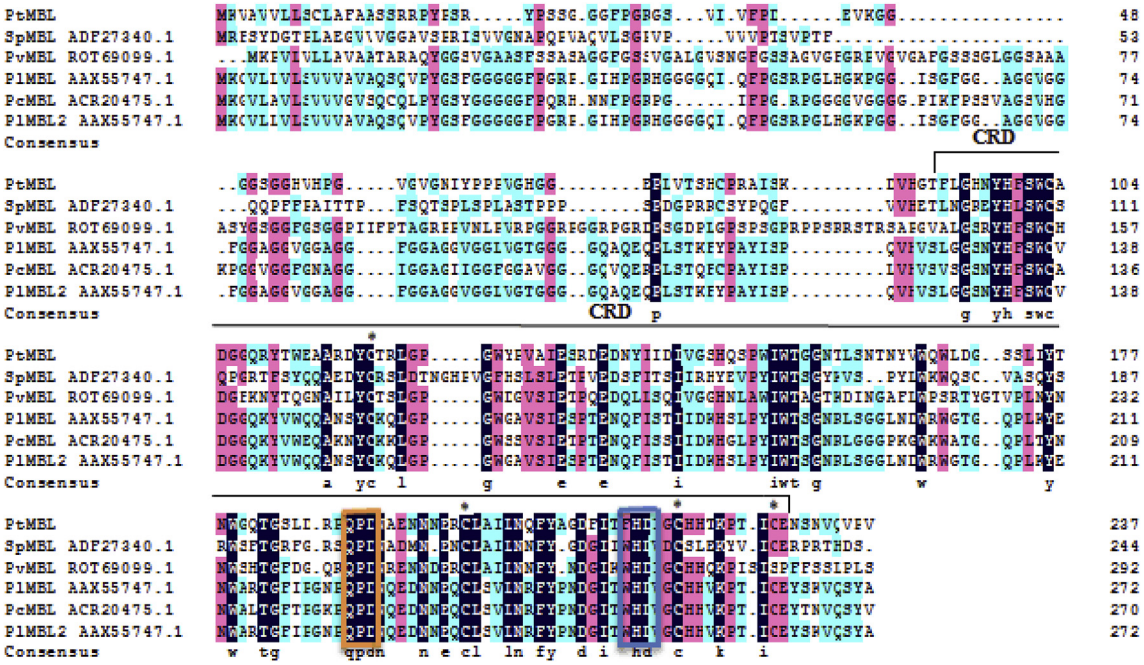

Fig. 2. Alignment of the amino acid sequence of single-CRD MBL of *P. trituberculatus* with other four crustacean MBLs. The QPD motif and FHD (WHD) motif is boxed in orange and blue. Four conserved cysteines are marked with asterisks. Numbers shown on the right of the sequences indicate the position of the amino acid residues. (For interpretation of the references to color in this figure legend, the reader is referred to the Web version of this article.)

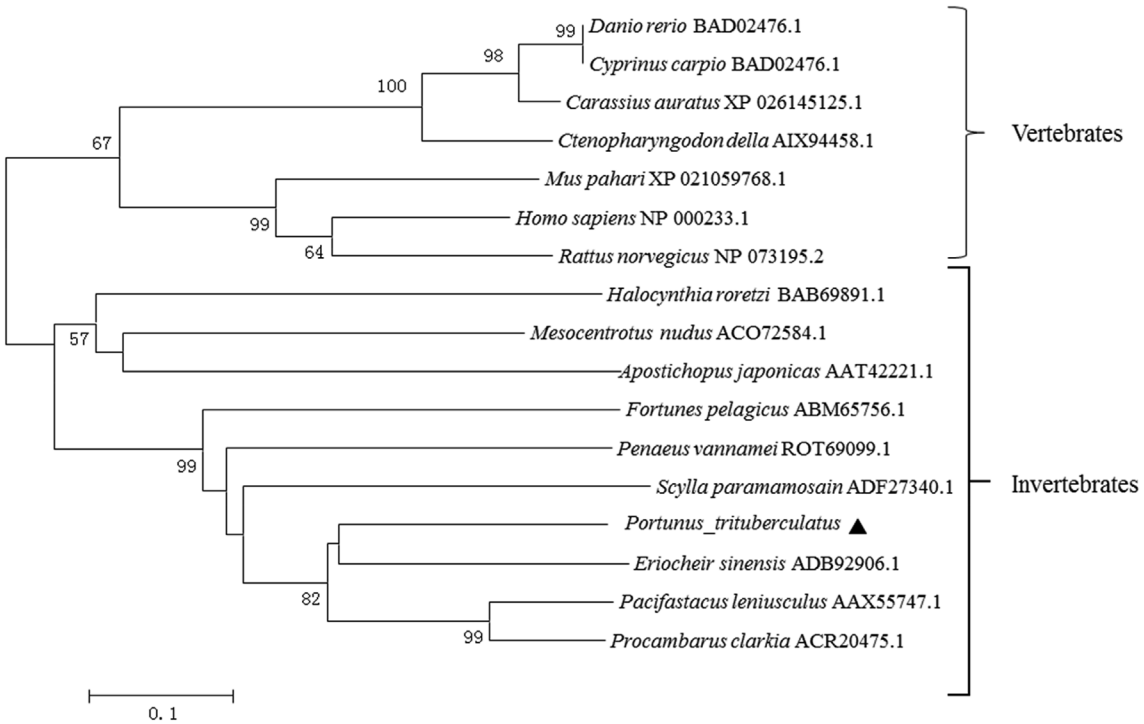

Fig. 3. Phylogenetic analysis of PtMBL and other MBLs. Neighbour-joining tree was constructed with Mega 7.0 software. Percentage bootstrap values are shown at branches. MBL from *P. trituberculatus* are shown with ▲. The bar (0.10) indicates the genetic distance.

transformed into competent *E. coli* BL21 (DE3) cells (Novagen) for overexpression. The pET-32a vector without insert fragment was selected as a negative control, which could express a thioredoxin (Trx) with 6 × His-tag in the prokaryotic expression system.

2.6. Expression and purification of recombinant PtMBL

Positive transformants of recombinant proteins and negative control were incubated in 200 mL LB medium (containing 100 mg/mL ampicillin) at 37 °C with shaking at 220 rpm. When the culture reached OD_{600} of 0.4–0.6, isopropyl-β-D-thiogalactosidase (IPTG) was added to the final concentration of 1 mM, and incubated for another 4 h under the same conditions. After centrifugation with 8000 g for 15 min at 4 °C, the cells were resuspended in buffer I (50 mM sodium phosphate, 300 mM NaCl, pH 7.0), sonicated at 4 °C for 30 min. The cell lysate and inclusion bodies were separated by the centrifugation as above. The

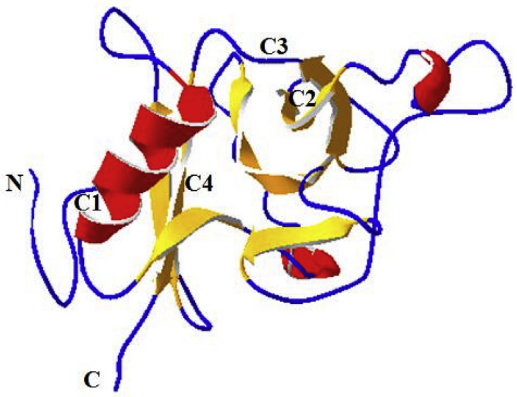

Fig. 4. The spatial structure of CRD in PtMBL predicted by SWISS-MODEL program. Where the α-helices are colored red, the β-stands are colored yellow, and the random coil is colored blue. There are four cysteines C1-C4 involved in forming disulfide bridges at the bases of the loops. (For interpretation of the references to color in this figure legend, the reader is referred to the Web version of this article.)

inclusion bodies were washed once with buffer I, twice with buffer II (50 mM sodium phosphate, 300 mM NaCl, 2 M urea, pH 7.0) and dissolved in buffer III (50 mM sodium phosphate, 300 mM NaCl, 8 M urea, pH 7.0). The recombinant PtMBL (rPtMBL) and rTrx proteins were purified by cobalt affinity chromatography (Clontech) as described by manufacturer under the denatured condition.

The purified proteins were refolded in gradient urea-TBS glycerol buffer (50 mM Tris-HCl, 50 mM NaCl, 10% glycerol, 1% glycine, 1 mM EDTA, 0.2 mM oxidized glutathione, 2 mM reduced glutathione 6, 4, 3, 2, 0 mM urea in each gradient, pH 8.0; each gradient at 4 °C for 8 h). The resultant proteins were separated by 12% sodium dodecyl sulphate-polyacrylamide gel electrophoresis (SDS-PAGE), and visualized with Coomassie brilliant blue R250. The purified protein solutions were concentrated with Microsep Advance Centrifugal Devices (10 kD, Pall corporation) based on the manufacturer's instructions. The concentration of rPtMBL and rTrx was measured by BCA (bicinchoninic acid) Protein Assay Kit (Beyotime), respectively.

2.7. Antimicrobial activity assay

Antimicrobial activity was measured against two Gram-negative bacteria *V. alginolyticus* and *Pseudomonas aeruginos*a, two Gram-positive bacteria *M. luteus* and *Staphylococcus aureus* and one fungus *P. pastoris* using a liquid phase assay modified from that of Rathinakumar et al. [27]. Briefly, bacteria and yeast were grown to mid-logarithmic phase and diluted with Tris-HCl buffer (50 mM, pH 8.0) to 10^3 CFU/mL. In sterile 96-well plate, 50 µl of recombinant proteins in 1/2-fold serial dilution with 50 mM Tris-HCl buffer (pH 8.0) were added into the wells. The wells with 50 µl of Tris- HCl (50 mM, pH 8.0) and 50 µl of rTrx diluted with Tris-HCl (50 mM, pH 8.0) were used as blank group and negative control, respectively. And then 50 µl of cell suspension (10^3 CFU/mL) were added into the wells and mixed. The 96-well plates were incubated at room temperature for 2 h, and 150 µl of medium was added, and then the mixtures were allowed to recover overnight. Absorbance at 600 nm for Gram-positive bacteria, 540 nm for Gram-negative bacteria or 560 nm for fungus of each well was determined using a precision microplate reader. The assay was performed with triplicates in three independent experiments.

The data were subjected to analysis of one way ANOVA using SPSS 16.0 and considered significant when $P < 0.05$. The minimum

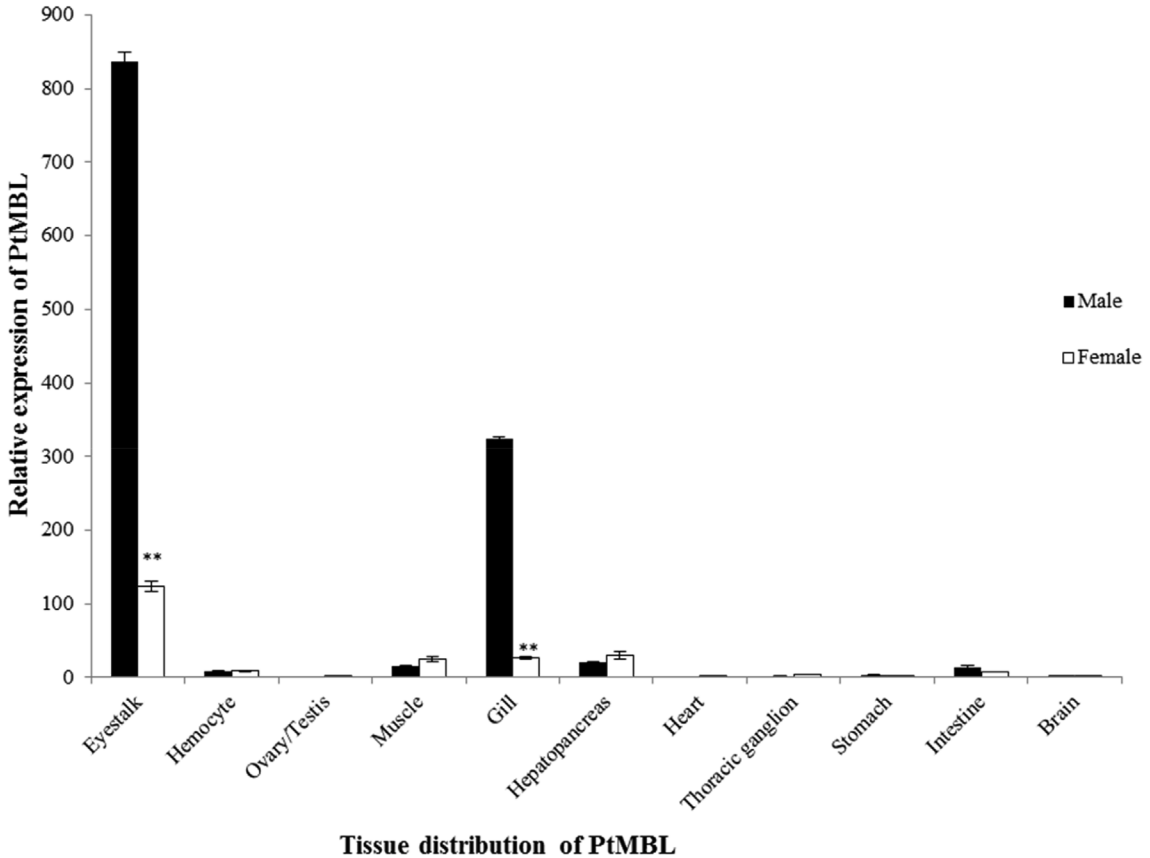

Fig. 5. Relative expression of PtMBL in different tissues of P. trituberculatus. The data determined by qRT-PCR. Each column represented the mean ± S.D. (n = 4). Significant differences between male and female were represented with asterisks (**$P < 0.01$).

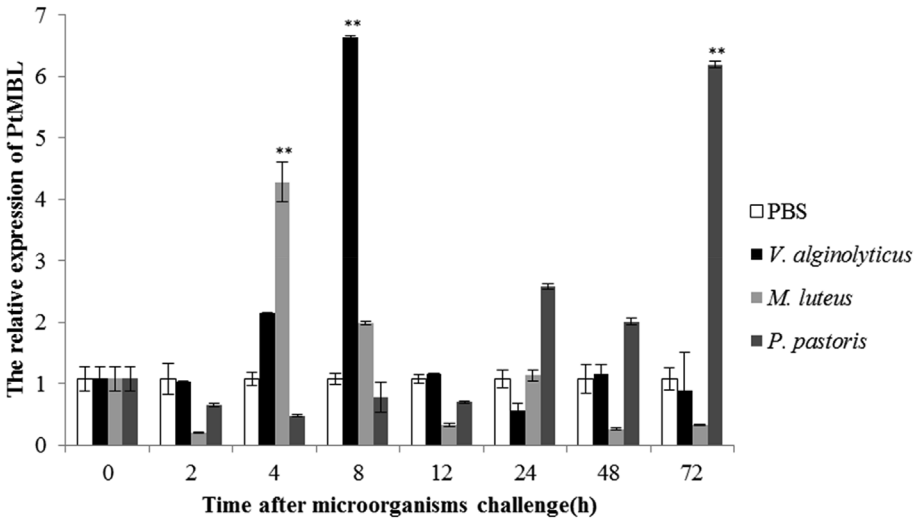

Fig. 6. Temporal expression profiles of PtMBL in hemocytes after challenged with *V. alginolyticus, M. luteus* and *P. pastoris* revealed by qRT-PCR. Each column represented the mean ± S.D. (n = 3). Samples challenged with PBS were adopted as control (white bars). The significant differences cross control in the same time of sampling were represented with asterisks (**$P < 0.01$).

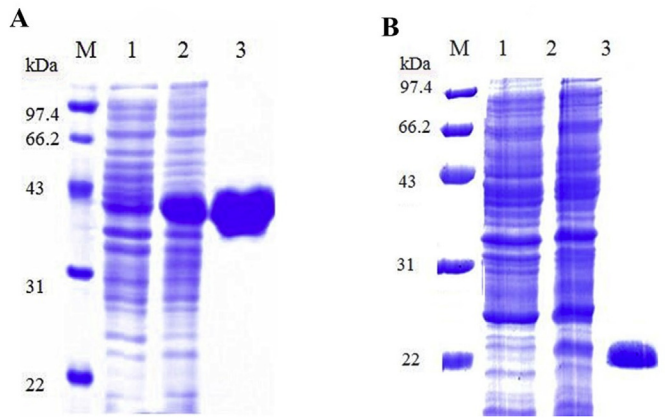

Fig. 7. SDS-PAGE analysis of rPtMBL (A) and rTrx (B). Lane M: protein molecular standard; lane A1: negative control for PtMBL without IPTG induction; LaneA2: IPTG induced PtMBL; LaneA3: purified PtMBL. lane B1: negative control for rTrx without induction; lane B2: IPTG induced rTrx; lane B3: purified rTrx.

Table 2
Antimicrobial activity expressed as minimal inhibition concentrations (MIC) of the recombinant proteins.

Microorganisms	MIC (μM)
Gram-negative bacteria	
Vibrio alginolyticus L59	0.81–1.61
Pseudomonas aeruginosa P25	< 0.81
Gram-positive bacteria	
Micrococcus luteus M2	0.81–1.61
Staphylococcus aureus S7	3.22–6.44
Fungus	
Pichia pastoris GS115	Na

inhibitory concentration (MIC) value was expressed as the range between the highest concentration of the protein where microbial growth was observed and the lowest concentration that caused 100% inhibition of microbial growth [28].

2.8. Assay of binding activity to microbes

The specific microbial-binding activity of PtMBL was tested against the above mentioned bacteria and fungus by the method described in previous report [29]. Gram-positive bacteria, Gram-negative bacteria and yeast were cultured at LB, TSB or YPD medium to the logarithmic growth phase respectively, and then fixed with 37% formaldehyde by gently shaking at 37 °C for 1 h to destroy the protease activity of microbes. 0.5 mL of the cells suspension (3×10^8 CFU/mL) with rTrx and 0.5 mL of purified rPtMBL protein (final concentration, 1.52 mg proteins) were mixed and incubated with gentle shaking at 4 °C for 30 min. After centrifugation at 2000*g* and 4 °C for 5 min, the supernatant was removed, and the cells were washed twice with PBS. Bound proteins were subsequently eluted with 1 × SDS-PAGE sample loading buffer. Microbes incubated with rTrx were used as control. The supernatant, washed and eluted fractions were run on 15% (w/v) SDS-PAGE.

2.9. Microbe agglutination assay

The agglutination assay was performed according to previous reports with some modifications [30,31]. The microbes were cultured in the corresponding growth medium to logarithmic growth phase and harvested by centrifugation at 2000*g* at 4 °C for 10 min. The pellets were washed three times with sterilized PBS, re-suspended in the PBS at a density of 10^8 cells/mL. The fluorescein isothiocyanate (FITC)-labeled Gram-negative bacteria *V. alginolyticus, P. aeruginosa*, Gram-positive bacteria *S. aureus*, *M. luteus* and fungi *P. pastoris* GS115 with slowly shaking overnight in the dark. The microbe was suspended in PBS at 1.0×10^8 cells/mL. Ten microliter microbe suspension was added to 25 μl PtMBL (25 nm mol L^{-1}) or 25 μl rTrx (25 nm mol L^{-1}) dissolved in Tris-HCl buffer. In order to determine whether PtMBL and microbial binding are Ca^{2+}-dependent, the microorganism solution was incubated with 25 μl PtMBL (25 nm mol L^{-1}) in the presence or absence of 10 mM $CaCl_2$. rTrx (25 nm mol L^{-1}) plus 10 mM $CaCl_2$ was used as a negative control. The mixtures were incubated at 17 °C for 2 h in the dark and 5 μl of cells were removed and observed by fluorescence microscopy.

2.10. Agglutination inhibition assay

To test the carbohydrate binding specificity of PtMBL, 15 μl of various carbohydrates were premixed with 25 μl of PtMBL and 10 mM $CaCl_2$ at room temperature for 30 min before adding the microbe suspension. The carbohydrates tested in this experiment included D-galactose (Sigma-Aldrich, USA), D-mannose (Sigma-Aldrich, USA), D-glucose (Sigma-Aldrich, USA), L-fucose (Sigma-Aldrich, USA) and sucrose (Sigma-Aldrich, USA) with a series of 2-fold diluted concentration ranging from 200 mmol L^{-1} to 25 mmol L^{-1}. The inhibitory effect was expressed as the minimum concentration required for complete inhibition of the agglutinating activity against FITC-labeled *V.*

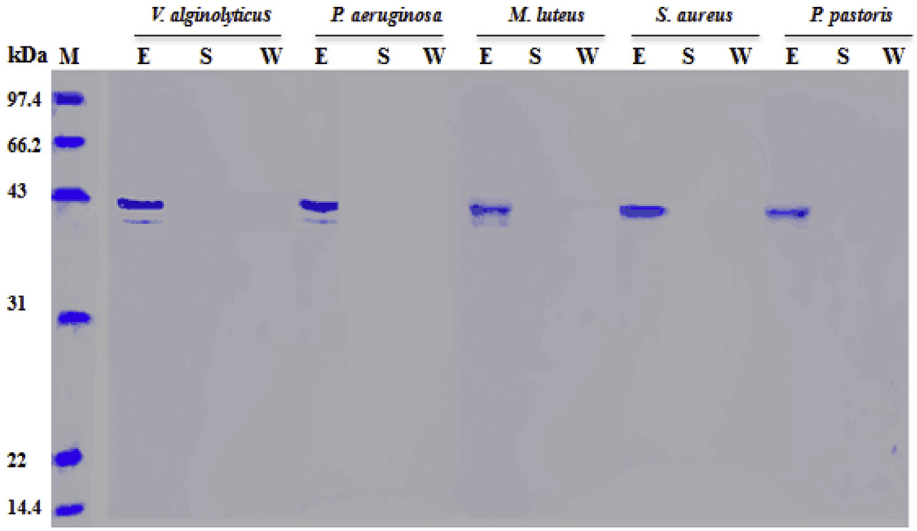

Fig. 8. Binding activity of the recombinant PtMBL to microorganisms. The recombinant proteins were incubated with formaldehyde-fixed microorganisms at 4 °C for 30 min. After incubation, the supernatants were separated by centrifugation. The pellets were washed with PBS buffer and the bound proteins were eluted with SDS-PAGE sample loading buffer. The eluted (E), supernatants (S) and washed (W) fractions were examined by SDS-PAGE.

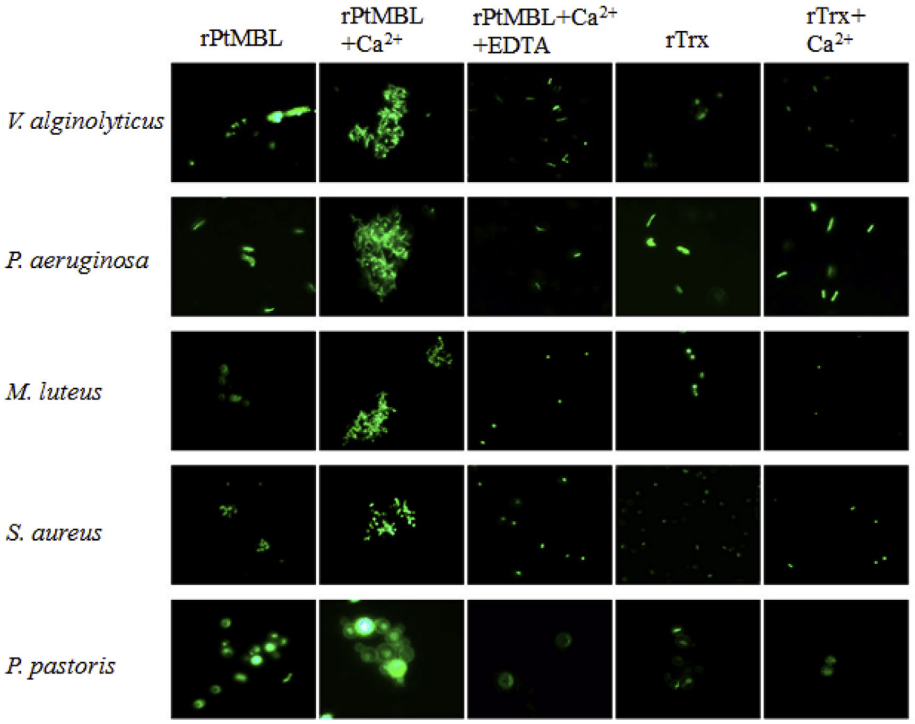

Fig. 9. Microbial agglutinating activity of rPtMBL against FITC-labeled *V. alginolyticus*, *P. aeruginosa*, *M. luteus*, *S. aureus* and *P. pastoris*. The concentration of rPtMBL, rTrx, $CaCl_2$ and EDTA were 25 nmol L^{-1}, 25 nmol L^{-1}, 10 mmol L^{-1} and 10 mmol L^{-1}, respectively.

alginolyticus.

3. Results

3.1. cDNA cloning and sequence analysis of PtMBL

The complete cDNA sequence of PtMBL gene was 1208 bp in length and deposited in GenBank under the accession number MK389481. The complete sequence of PtMBL consisted of a 5′-untranslated region (UTR) of 40 bp, an open reading frame (ORF) of 732 bp, and a 3′ UTR of 436 bp with the polyadenylation signal (AATAAA) and poly (A) tail. The nucleotide and deduced amino acid sequences are shown in Fig. 1. The putative signal peptide was identified with predicted cleavage sites between Ser^{16}-Ser^{17}. A single CRD domain and four conserved cysteine residues forming two disulfide-bonds (Cys^{119}-Cys^{228}, Cys^{200}-Cys^{220}) were detected in PtMBL. The estimated molecular weight of mature PtMBL (227 amino acids) was 24.87 kDa and its theoretical isoelectric point was 5.95.

3.2. Homologous and phylogenetic analysis of PtMBL

BLAST analysis revealed the deduced amino acid sequence of PtMBL matched a variety of MBLs previously submitted to GenBank. However, the sequence similarities were relatively low. PtMBL displayed 54% amino acid identity with MBL from *Procambarus clarkii* (PcMBL, ACR20475.1) and MBL from *P. leniusculus* (PlMBL, AAX55747.1), and 43% with MBL from *P. vannamei* (PvMBL, ROT75937.1). Multiple sequence alignment showed that all these MBLs had Ca^{2+}-binding motif FHD and sugar recognition motif QPD in the single CRD domain (Fig. 2). A phylogenetic tree derived from 17 amino acid sequences of

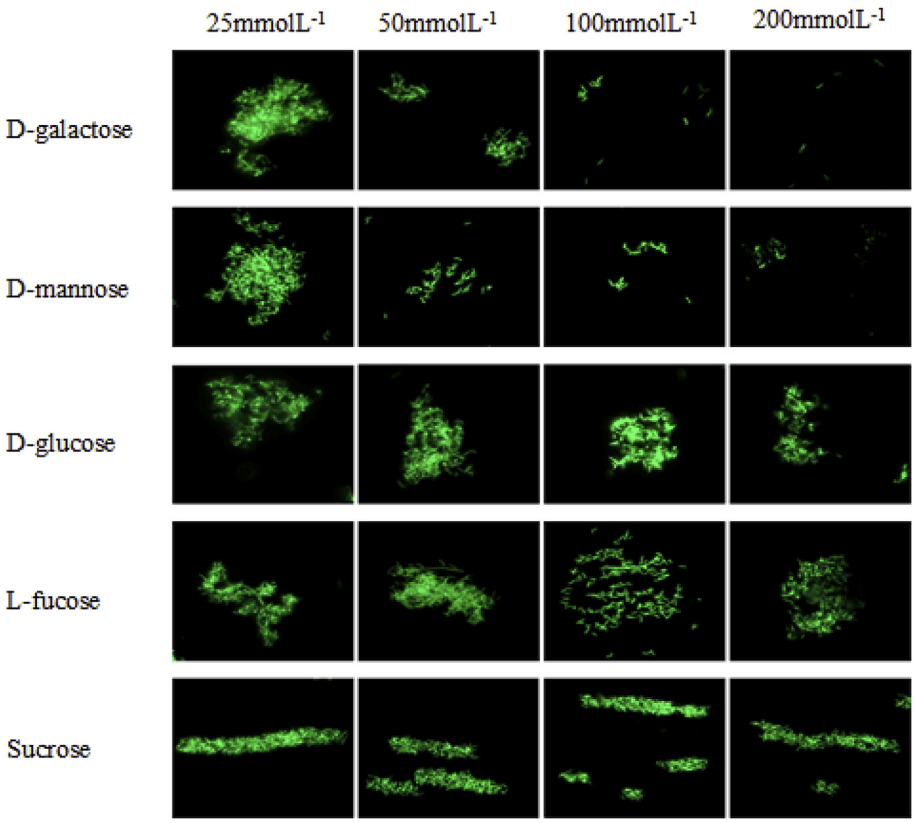

Fig. 10. Inhibition of agglutinating activity of rPtMBL against *V. alginolyticus* by various compounds. FITC-labeled *V. alginolyticus* was incubated in Tris-HCl buffer with 25 nmol L^{-1} rPtMBL and 10 mmol L^{-1} $CaCl_2$.

MBLs was illustrated in Fig. 3. PtMBL were clustered with MBLs from other crustaceans, and then had a closer relationship with other invertebrates MBLs. The MBLs from mammals and fish were clustered into the distinct vertebrate group.

3.3. The potential tertiary structure of CRD in PtMBL

The predicted structure of CRD in PtMBL contained six β-stands located between three α-helices. Four conserved cysteines (C1–C4) formed two disulfide bridges at the bases of the loops. C1 and C4 linked the whole domain loop, while C2 and C3 linked the long loop region (Fig. 4).

3.4. Tissue distribution of PtMBL transcripts

The mRNA transcripts of PtMBL were detected in all examined tissues, including hemocytes, gill, hepatopancreas, eyestalk, muscle, heart, intestine, stomach, thoracic ganglion, gonads and brain (Fig. 5). The highest level of PtMBL transcripts was detected in eyestalk, followed by gill, hepatopancreas, muscle and hemocytes. The expression of PtMBL in eyestalk and gill of male crabs was significantly higher than those in female crabs ($P < 0.01$).

3.5. Temporal change of PtMBL transcripts after bacterial and fungal challenge

The temporal mRNA expression of PtMBL in hemocytes post *V. alginolyticus*, *M. luteus* and *P. pastoris* challenge was shown in Fig. 6. After *V. alginolyticus* challenge, the expression of PtMBL was induced and reached the peak at 8 h post-injection, which was 6.6-fold to that in the control group ($P < 0.01$). Then, the PtMBL expression decreased sharply and recovered to the control level from 12 to 72 h post-injection. The expression of PtMBL was decreased at 2 h post *M. luteus* infection, and then increased significantly at 4 h post-injection and was 4.3-fold higher than that in the control group ($P < 0.01$). As time progressed, the expression level of PtMBL mRNA in the challenge group decreased gradually and reached the lowest level at 48 h post-injection. During the first 12 h after *P. pastoris* challenge, the expression of PtMBL was decreased, and then upregulated at 24 h post-injection, and reached the peak at 72 h post-injection (5.76-fold to that in the control group, $P < 0.01$).

3.6. Expression and purification of the recombinant PtMBL protein

The recombinant plasmid pET-32a-PtMBLwas transformed and expressed in *E. coli* BL21 (DE3)-pLysS. The induced rPtMBL was mainly expressed as inclusion bodies with extra His-tag and Trx-tag (about 20 kDa) to the N-terminus (Fig. 7B, lanes 3). It had a distinct band with molecular weight of about 43 kDa (Fig. 7A, lane 3) which was in accordance with the predicted molecular mass of fusion protein. The concentration of the rPtMBL and rTrx proteins was 1.52 mg/mL and 1.20 mg/mL, respectively.

3.7. Antimicrobial activity of rPtMBL

The antimicrobial activity of the purified rPtMBL protein against several stains of Gram-negative, Gram-positive bacteria and fungus was determined by a liquid growth inhibition assay (Table 2). The rPtMBL protein could inhibit all the tested Gram-negative bacteria *V. alginolyticus* and *P. aeruginosa*, Gram-positive bacteria *M. luteus* and *S. aureus*. The highest antibacterial activity was against *P. aeruginosa* with MIC value of less than 0.81 μM. No obvious inhibitory activity was detected against fungus *P. pastoris*.

MIC are expressed as the interval a-b, where a was the highest concentration tested at which microorganisms are growing ($P > 0.05$) and b was the lowest concentration that cause 100% growth inhibition

($P < 0.05$). Na: indicated no antimicrobial activity.

3.8. Binding activity to microbes

The microbial-binding assay revealed that rPtMBL was detected in the eluted fractions, whereas no band was detected in the supernatant or washed fractions (Fig. 8). However, rTrx showed clear bands in the supernatant fractions, and no or weak band in the precipitate fractions (data not shown). This results indicated rPtMBL could strongly bind to the Gram-negative bacteria *V. alginolyticus* and *P. aeruginosa,* Gram-positive bacteria *M. luteu* and *S. aureus*, and yeast *P. pastoris*, while rTrx had no microbes binding ability.

3.9. Microbe agglutination assay

The microbial agglutinating activity of rPtMBL was determined by incubation with FITC-labeled microbes. The rPtMBL protein could significantly agglutinate all the tested microbes in the presence of Ca^{2+}. However, it exhibited no agglutination activity in the absence of Ca^{2+} and in the presence of EDTA and Ca^{2+}. No agglutination was observed in rTrx groups (Fig. 9). Moreover, the agglutinating activity of rPtMBL towards *V. alginolyticus* was inhibited after the addition of 100 mmol L^{-1} D-galactose and 100 mmol L^{-1} D-mannose, while no significant change of this agglutinating activity was observed after the incubation of other carbohydrates even at their maximum tested concentration (Fig. 10).

4. Discussion

Mannose-binding lectin (MBL) is an important PRR in the first line defense against infection of pathogens by recognizing and binding with the PAMPs of the microbes [1,32,33]. In the present study, PtMBL shared the conserved signal peptide and CRD domain with other identified crustacean MBLs [34,35], suggesting it is a secreted carbohydrate-recognition protein. Unlike vertebrate MBLs, PtMBL lacks a collagen-like domain consisting of tandem repeats of Gly-X-Y triplet sequences. It is similar to the MBLs from some invertebrates, such as GBL from ascidian *Hyalella azteca*, CgCLec-2 from oyster *Crassostrea gigas*, galNAc from tunicate *Styela plicata* and CioMBL from urochordate species *Ciona intestinalis* [36–38]. As suggested by Li et al. [39], we also speculate that the predicted coiled-coil region in the N-terminal region of PtMBL is similar to the Gly-X-Y repeats in vertebrate MBL and α helix structure in ascidian GBL that could interact with MASPs to form a complex. The phylogenetic results further show that PtMBL is clustered with those from invertebrate MBLs. The sequence similarity and characteristic in domain structure indicate that PtMBL is a new member of the collectin family in crab.

Most MBLs are mainly detected in hepatopancreas and hemocytes [17,18], however, in our study, the eyestalk and gill are the main expression tissues of PtMBL. Gill is believed to be the first defense line against invading microbes in fish and crustaceans [40]. The crustacean eyestalk is a major neuroendocrine organ complex [41]. The highest expression level of PtMBL in eyestalk implies PtMBL might be involved in the multiple biological processes. Interestingly, the expression of PtMBL in eyestalk and gill is significantly higher in males than in females, suggesting the sex differences might exist in immune defense of crab. Similar results have been reported in PtgC1qR of *P. trituberculatus*, with higher expression in hepatopancreas and gonads of females than males [42]. And eight up-regulated pattern recognition receptors (PRRs) in male *Eriocheir sinensis* were found in transcriptome analysis [43]. PtMBL mRNA transcripts increased significantly in a short time after *V. alginolyticus* and *M. luteus* and challenge, which is similar to those reported in Pc-DWD from *P. clarkia* [44] and EsGal from *E. sinensis* [45]. However, the expression of PtMBL showed no significant change during the 48 h after *P. pastoris* challenge. These results suggest PtMBL could respond to the invading bacteria more quickly than fungus.

Accumulating evidences demonstrated that some C-type lectins exhibited growth suppression activity against microbes [46]. MrMBL-N20 and MrMBL-C16 peptides, deriving from MrMBL of prawn *M. rosenbergii* exhibited significant inhibitory effect on the growth of many Gram-negative and Gram-positive bacteria [19]. EsLecA and EsLecG from Chinese Mitten Crab *E. sinensis* showed antimicrobial activity toward *S. aureus*, *E. coli* and *P. pastoris* [5]. In the present study, the rPtMBL protein also exhibited strong antimicrobial activities against both Gram-negative and Gram-positive bacteria, indicating PtMBL is a potential antibacterial protein. Moreover, rPtMBL has a broad spectrum of binding activities towards all the tested bacteria and fungus. Similar microbial binding activities have also reported in rSpCTL-B from *Scylla paramamosain*, rEsLecF from *E. sinensis* [5,46–48]. However, it is different with the results that FcLec4 from *F. chinensis* could not bind to Klebsiella pneumonia [49] and Pc-Lec1 from *Procambarus clarkia* almost could not bind to *P. aeruginosa, Bacillus megaterium* or *B.cereus* [50].

In invertebrate immune defense system, agglutination is one of the important responses to recognize the foreign pathogens thereby mediating further immune activities [51]. In this study, rPtMBL exhibited remarkable agglutination activity against Gram-negative bacteria, Gram-positive bacteria and fungus with the presence of Ca^{2+}. This is in accordance with the previous reports in other invertebrates that MBL is able to recognize bacteria via the CRD domain in presence of Ca^{2+} [52,53]. The results indicate that PtMBL is involved in immune defense against a broad-spectrum of microbes by recognizing and binding to their surface.

As the classical motifs, QPD and EPN have been already found in many vertebrates, which are considered to specifically bind galactose and mannose, respectively [38,54]. However, in this study, rPtMBL with QPD motif could not only bind D-galactose but also D-mannose by agglutination inhibition assay. Similar results have been found in other invertebrates, for example, in scallop *Argopecten irradian*, AiCTL-3 with the EPN motif can bind D-mannose and D-galactose [54], and in abalone *H. laevigata*, perlucin with the QPD motif can recognize and bind D-galactose, D-mannose and D-glucose [55]. Further, the EPN and QPD motifs in CioMBLs from *C. intestinalis* were both found to bind to mannose [38]. These recognition patterns suggest that the QPD or EPN motif in invertebrate C-type lectins have more powerful capability to recognize various pathogens than that in vertebrates [12].

In summary, a novel PtMBL containing a single CRD with a QPD motif was identified in the crab *P. trituberculatus*. PtMBL is highly expressed in eyestalk and could be quickly induced by bacterial challenge. In addition to binding and agglutinating activities to various microbes, the recombinant PtMBL could inhibit the growth of Gram-negative bacteria and Gram-positive bacteria. All these results demonstrate that PtMBL may involve in immune recognition and pattern elimination in the innate immunity of *P. trituberculatus*. This study provided new insights into understanding the functions of MBL in crustaceans.

Acknowledgments

We are grateful to all the laboratory members for technical advice and helpful discussions. This research was supported by National Key R &D Program of China (2018YFD0900303), National Natural Science Foundations of China (41776159), Scientific and Technological Innovation Project of Qingdao National Laboratory for Marine Science and Technology (2015ASKJ02) and Natural Science Foundation of Shandong Province (ZR2017QD001).

References

[1] S. Kurata, S. Ariki, S.-i. Kawabata, Recognition of pathogens and activation of immune responses in *Drosophila* and horseshoe crab innate immunity, Immunobiology 211 (2006) 237–249.
[2] S. Young Lee, K. Söderhäll, Early events in crustacean innate immunity, Fish

Shellfish Immunol. 12 (2002) 421–437.
[3] S. Akira, S. Uematsu, O. Takeuchi, Pathogen recognition and innate immunity, Cell 124 (2006) 783–801.
[4] T. Hoi-Tung Ma, J.A.H. Benzie, J.-G. He, S.-M. Chan, PmLT, a C-type lectin specific to hepatopancreas is involved in the innate defense of the shrimp *Penaeus monodon*, J. Invertebr. Pathol. 99 (2008) 332–341.
[5] X.-K. Jin, S. Li, X.-N. Guo, L. Cheng, M.-H. Wu, S.-J. Tan, Y.-T. Zhu, A.-Q. Yu, W.-W. Li, Q. Wang, Two antibacterial C-type lectins from crustacean, *Eriocheir sinensis*, stimulated cellular encapsulation in vitro, Dev. Comp. Immunol. 41 (2013) 544–552.
[6] M.E. Taylor, P.M. Brickell, R.K. Craig, J.A. Summerfield, Structure and evolutionary origin of the gene encoding a human serum mannose-binding protein, Biochem. J. 262 (1989) 763.
[7] K. Sastry, K. Zahedi, J.M. Lelias, A.S. Whitehead, R.A. Ezekowitz, Molecular characterization of the mouse mannose-binding proteins. The mannose-binding protein A but not C is an acute phase reactant, J. Immunol. 147 (1991) 692.
[8] Dalgaard Laursen, Lim Thiel, M. Juul Jensen, Hamana Takahashi, Jensenius Kawakami, Cloning and sequencing of a cDNA encoding chicken mannan-binding lectin (MBL) and comparison with mammalian analogues, Immunology 93 (1998) 421–430.
[9] Y. Dang, X. Meng, S. Wang, L. Li, M. Zhang, M. Hu, X. Xu, Y. Shen, L. Lv, R. Wang, J. Li, Mannose-binding lectin and its roles in immune responses in grass carp (*Ctenopharyngodon idella*) against *Aeromonas hydrophila*, Fish Shellfish Immunol. 72 (2018) 367–376.
[10] F. Zheng, M. Asim, J. Lan, L. Zhao, S. Wei, N. Chen, X. Liu, Y. Zhou, L. Lin, Molecular cloning and functional characterization of mannose receptor in zebra fish (*Danio rerio*) during infection with *Aeromonas sobria*, Int. J. Mol. Sci. 16 (2015).
[11] U. Holmskov, R. Malhotra, R.B. Sim, J.C. Jensenius, Collectins: collagenous C-type lectins of the innate immune defense system, Immunol. Today 15 (1994) 67–74.
[12] A.N. Zelensky, J.E. Gready, The C-type lectin-like domain superfamily, FEBS J. 272 (2005) 6179–6217.
[13] T. Fujita, M. Matsushita, Y. Endo, T. Fujita, M. Matsushita, Y. Endo, The lectin-complement pathway—its role in innate immunity and evolution, Immunol. Rev. 198 (2004) 185–202.
[14] W.I. Weis, K. Drickamer, W.A. Hendrickson, Structure of a C-type mannose-binding protein complexed with an oligosaccharide, Nature 360 (1992) 127.
[15] K. Drickamer, Engineering galactose-binding activity into a C-type mannose-binding protein, Nature 360 (1992) 183.
[16] M. Huang, L. Wang, H. Zhang, C. Yang, R. Liu, J. Xu, Z. Jia, L. Song, The sequence variation and functional differentiation of CRDs in a scallop multiple CRDs containing lectin, Dev. Comp. Immunol. 67 (2017) 333–339.
[17] X. Man, X.-T. Pan, H.-W. Zhang, Y. Wang, X.-C. Li, X.-W. Zhang, A mannose receptor is involved in the anti-*Vibrio* defense of red swamp crayfish, Fish Shellfish Immunol. 82 (2018) 258–266.
[18] C. Wu, W. Charoensapsri, S. Nakamura, A. Tassanakajon, I. Söderhäll, K. Söderhäll, An MBL-like protein may interfere with the activation of the proPO-system, an important innate immune reaction in invertebrates, Immunobiology 218 (2013) 159–168.
[19] J. Arockiaraj, M.K. Chaurasia, V. Kumaresan, R. Palanisamy, R. Harikrishnan, M. Pasupuleti, M. Kasi, *Macrobrachium rosenbergii* mannose binding lectin: Synthesis of MrMBL-N20 and MrMBL-C16 peptides and their antimicrobial characterization, bioinformatics and relative gene expression analysis, Fish Shellfish Immunol. 43 (2015) 364–374.
[20] Z.-Y. Zhao, Z.-X. Yin, X.-P. Xu, S.-P. Weng, X.-Y. Rao, Z.-X. Dai, Y.-W. Luo, G. Yang, Z.-S. Li, H.-J. Guan, S.-D. Li, S.-M. Chan, X.-Q. Yu, J.-G. He, A novel C-type lectin from the shrimp *Litopenaeus vannamei*; possesses anti-white spot syndrome virus activity, J. Virol. 83 (2009) 347.
[21] W.-T. Xu, X.-W. Wang, X.-W. Zhang, X.-F. Zhao, X.-Q. Yu, J.-X. Wang, A new C-type lectin (FcLec5) from the Chinese white shrimp *Fenneropenaeus chinensis*, Amino Acids 39 (2010) 1227–1239.
[22] P. Runsaeng, S. Thepnarong, O. Rattanaporn, P. Utarabhand, Cloning and the mRNA Expression of a C-type Lectin with One Carbohydrate Recognition Domain from *Fenneropenaeus Merguiensis* in Response to Pathogenic Inoculation, (2015).
[23] Fisheries Bureau of Agriculture Ministry of China, (2017).
[24] J. Rodriguez, V. Boulo, E. Mialhe, E. Bachere, Characterisation of shrimp haemocytes and plasma components by monoclonal antibodies, J. Cell Sci. 108 (1995) 1043.
[25] Z. Cui, Y. Liu, W. Luan, Q. Li, D. Wu, S. Wang, Molecular cloning and characterization of a heat shock protein 70 gene in swimming crab (*Portunus trituberculatus*), Fish Shellfish Immunol. 28 (2010) 56–64.
[26] K.J. Livak, T.D. Schmittgen, Analysis of relative gene expression data using real-time quantitative PCR and the $2-\Delta\Delta CT$ method, Methods 25 (2001) 402–408.
[27] R. Rathinakumar, W.F. Walkenhorst, W.C. Wimley, Broad-spectrum antimicrobial peptides by rational combinatorial design and high-throughput screening: the importance of interfacial activity, J. Am. Chem. Soc. 131 (2009) 7609–7617.
[28] P. Casteels, C. Ampe, F. Jacobs, P. Tempst, Functional and chemical characterization of Hymenoptaecin, an antibacterial polypeptide that is infection-inducible in the honeybee (*Apis mellifera*), J. Biol. Chem. 268 (1993) 7044–7054.
[29] S.Y. Lee, K. Söderhäll, Characterization of a pattern recognition protein, a masquerade-like protein, in the freshwater crayfish *Pacifastacus leniusculus*, J. Immunol. 166 (2001) 7319.
[30] Z. Wang, S. Zhang, The role of lysozyme and complement in the antibacterial activity of zebrafish (*Danio rerio*) egg cytosol, Fish Shellfish Immunol. 29 (2010) 773–777.
[31] X.-Q. Yu, H. Gan, M.R. Kanost, Immulectin, an inducible C-type lectin from an insect, *Manduca sexta*, stimulates activation of plasma prophenol oxidase, Insect Biochem. Mol. Biol. 29 (1999) 585–597.
[32] M.W. Turner, The role of mannose-binding lectin in health and disease, Mol. Immunol. 40 (2003) 423–429.
[33] A. Agah, M.C. Montalto, K. Young, G.L. Stahl, Isolation, cloning and functional characterization of porcine mannose-binding lectin, Immunology 102 (2001) 338–343.
[34] S. Sricharoen, J.J. Kim, S. Tunkijjanukij, I. Söderhäll, Exocytosis and proteomic analysis of the vesicle content of granular hemocytes from a crayfish, Dev. Comp. Immunol. 29 (2005) 1017–1031.
[35] A.V. Kuballa, A. Elizur, Differential expression profiling of components associated with exoskeletal hardening in crustaceans, BMC Genomics 9 (2008) 575-575.
[36] T. Fujita, M. Matsushita, Y. Endo, The lectin-complement pathway – its role in innate immunity and evolution, Immunol. Rev. 198 (2004) 185–202.
[37] S.V. Nair, S. Pearce, P.L. Green, D. Mahajan, R.A. Newton, D.A. Raftos, A collectin-like protein from tunicates, Comp. Biochem. Physiol. B Biochem. Mol. Biol. 125 (2000) 279–289.
[38] M.-O. Skjoedt, Y. Palarasah, K. Rasmussen, L. Vitved, J. Salomonsen, A. Kliem, S. Hansen, C. Koch, K. Skjodt, Two mannose-binding lectin homologues and an MBL-associated serine protease are expressed in the gut epithelia of the urochordate species *Ciona intestinalis*, Dev. Comp. Immunol. 34 (2010) 59–68.
[39] H. Li, H. Zhang, S. Jiang, W. Wang, L. Xin, H. Wang, L. Wang, L. Song, A single-CRD C-type lectin from oyster *Crassostrea gigas* mediates immune recognition and pathogen elimination with a potential role in the activation of complement system, Fish Shellfish Immunol. 44 (2015) 566–575.
[40] D. Weihrauch, M.P. Wilkie, P.J. Walsh, Ammonia and urea transporters in gills of fish and aquatic crustaceans, J. Exp. Biol. 212 (2009) 1716.
[41] D. Weihrauch, M.P. Wilkie, P.J. Walsh, Ammonia and Urea Transporters in Gills of Fish and Aquatic Crustaceans, (2009).
[42] J. Ning, Y. Liu, F. Gao, H. Liu, Z. Cui, Characterization and functional analysis of a novel gC1qR in the swimming crab *Portunus trituberculatus*, Fish Shellfish Immunol. 84 (2019) 970–978.
[43] Y. Liu, M. Hui, Z. Cui, D. Luo, C. Song, Y. Li, L. Liu, Comparative transcriptome analysis reveals sex-biased gene expression in juvenile Chinese mitten crab *Eriocheir sinensis*, PLoS One 10 (2015) e0133068.
[44] H.-W. Zhang, X. Man, Y. Wang, Q.-S. Song, D. Stanley, K.-M. Hui, X.-W. Zhang, Characterization of a double WAP domain-containing protein from the red swamp crayfish *Procambarus clarkii*, Fish Shellfish Immunol. 71 (2017) 329–337.
[45] M. Wang, L. Wang, M. Huang, Q. Yi, Y. Guo, Y. Gai, H. Wang, H. Zhang, L. Song, A galectin from *Eriocheir sinensis* functions as pattern recognition receptor enhancing microbe agglutination and haemocytes encapsulation, Fish Shellfish Immunol. 55 (2016) 10–20.
[46] B.N. Lillie, A.S. Brooks, N.D. Keirstead, M.A. Hayes, Comparative genetics and innate immune functions of collagenous lectins in animals, Vet. Immunol. Immunopathol. 108 (2005) 97–110.
[47] X. Wei, L. Wang, W. Sun, M. Zhang, H. Ma, Y. Zhang, X. Zhang, S. Li, C-type lectin B (SpCTL-B) regulates the expression of antimicrobial peptides and promotes phagocytosis in mud crab *Scylla paramamosain*, Dev. Comp. Immunol. 84 (2018) 213–229.
[48] X.-K. Jin, X.-N. Guo, S. Li, M.-H. Wu, Y.-T. Zhu, A.-Q. Yu, S.-J. Tan, W.-W. Li, P. Zhang, Q. Wang, Association of a hepatopancreas-specific C-type lectin with the antibacterial response of *Eriocheir sinensis*, PLoS One 8 (2013) e76132-e76132.
[49] X.-W. Wang, X.-W. Zhang, W.-T. Xu, X.-F. Zhao, J.-X. Wang, A novel C-type lectin (FcLec4) facilitates the clearance of *Vibrio anguillarum* in vivo in Chinese white shrimp, Dev. Comp. Immunol. 33 (2009) 1039–1047.
[50] X.-W. Zhang, X.-W. Wang, C. Sun, X.-F. Zhao, J.-X. Wang, C-type lectin from red swamp crayfish *Procambarus clarkii* participates in cellular immune response, Arch. Insect Biochem. Physiol. 76 (2011) 168–184.
[51] C.G.C. Jacobs, H.P. Spaink, M. van der Zee, The extraembryonic serosa is a frontier epithelium providing the insect egg with a full-range innate immune response, eLife 3 (2014) e04111.
[52] Y.-y. Sun, L. Liu, J. Li, L. Sun, Three novel B-type mannose-specific lectins of *Cynoglossus semilaevis* possess varied antibacterial activities against Gram-negative and Gram-positive bacteria, Dev. Comp. Immunol. 55 (2016) 194–202.
[53] X. Yin, L. Mu, Y. Li, L. Wu, Y. Yang, X. Bian, B. Li, S. Liao, Y. Miao, J. Ye, Identification and characterization of a B-type mannose-binding lectin from Nile tilapia (*Oreochromis niloticus*) in response to bacterial infection, Fish Shellfish Immunol. 84 (2019) 91–99.
[54] M. Huang, X. Song, J. Zhao, C. Mu, L. Wang, H. Zhang, Z. Zhou, X. Liu, L. Song, A C-type lectin (AiCTL-3) from bay scallop *Argopecten irradians* with mannose/galactose binding ability to bind various bacteria, Gene 531 (2013) 31–38.
[55] K. Mann, I.M. Weiss, S. André, H.-J. Gabius, M. Fritz, The amino-acid sequence of the abalone (*Haliotis laevigata*) nacre protein perlucin, Eur. J. Biochem. 267 (2000) 5257–5264.